

Adsorption of Aqueous Uranyl Complexes onto *Bacillus subtilis* Cells

DREW GORMAN-LEWIS,*
PATRICIA E. ELIAS, AND
JEREMY B. FEIN

Department of Civil Engineering and Geological Sciences,
University of Notre Dame, Notre Dame, Indiana 46556

In oxygenated, CO₂-rich systems, negatively charged uranyl complexes dominate the aqueous uranium speciation, and it is commonly assumed that these complexes exhibit negligible adsorption onto negatively charged surfaces such as bacteria. We measured the adsorption of 4.2×10^{-6} M aqueous uranium onto *Bacillus subtilis* from pH 1.5 to 9 and with wet weight bacterial concentrations from 0.125 to 0.5 g/L. Experiments were performed in the presence and absence of dissolved CO₂, and additional experiments were performed in the presence of dissolved CO₂ and Ca. We observed extensive uranium adsorption onto the bacterial surface under all conditions. Thermodynamic modeling of the data suggests that uranyl-hydroxide, uranyl-carbonate, and calcium-uranyl-carbonate species each can form stable surface complexes on the bacterial cell wall. These results could dramatically alter predictions of uranium mobility in near-surface environments.

Introduction

The release of radionuclides into the environment from mining activities, nuclear weapons, and nuclear energy production and the storage of radioactive waste has focused research on the development of accurate and adaptable tools to predict the fate and transport of these contaminants in the subsurface (1). The high solubility and structural complexity of U(VI) mineral phases, and the complex speciation of aqueous uranium, make the prediction of uranium mobility difficult. The adsorption of aqueous uranium species onto mineral and bacterial surfaces can control the speciation, and hence the mobility, of uranium in the subsurface (2, 3). Considerable attention has been paid to uranium adsorption onto a range of mineral surfaces of environmental interest. However, very little research has focused on uranium adsorption onto bacteria, especially under the circumneutral pH conditions where the aqueous uranium speciation is so complex.

Under oxidizing conditions, uranium is present in aqueous solutions as the highly soluble uranyl ion, UO₂⁺². Because the uranyl ion forms a number of stable hydroxide and carbonate complexes in the pH range 5–10, the circumneutral uranium adsorption behavior can be complicated. Above pH 5, neutral and negatively charged uranyl-carbonates dominate the aqueous uranium speciation, typically causing a significant decrease in uranium adsorption onto mineral surfaces (4–7). In groundwater systems, high calcium

concentrations are common, and an aqueous calcium-uranyl-carbonate complex has been identified and can dominate uranium speciation in mid- to high-pH solutions. The tendency for these uranyl complexes to remain in solution has led to the common assumption that such aqueous complexation causes a high degree of uranium mobility (8, 9). Furthermore, the presumed mobility of these uranyl complexes represents the basis of proposed remediation strategies that rely on the formation of uranyl-carbonate complexes to mobilize uranium (10–12). Although there is some evidence that uranyl-carbonate complexes can adsorb onto mineral surfaces (13–16), the assumptions of uranium mobility persist, and there have been no studies that have determined whether these complexes adsorb to any significant extent onto negatively charged bacterial surfaces.

Most previous studies of bacterial surface uranyl adsorption have focused on low pH conditions where UO₂⁺² is the predominant aqueous uranium species. These studies typically model adsorption by invoking a bulk partitioning approach that cannot be extrapolated to conditions that differ significantly from those investigated in the laboratory (17, 18). Surface complexation approaches offer a more mechanistic and flexible approach. Fowle et al. (19) used a surface complexation approach to model their measurements of low pH uranium adsorption onto the Gram-positive bacterial species *Bacillus subtilis*, ascribing the observed adsorption behavior to UO₂⁺² binding onto two distinct types of bacterial surface sites. Kelly et al. (20) confirmed the stoichiometry proposed by Fowle et al. through an X-ray absorption spectroscopy study performed on similar uranium-*B. subtilis* samples. Haas et al. (21) also applied surface complexation modeling to open atmosphere measurements of uranyl adsorption onto the Gram-negative bacterium *Shewanella putrefaciens*. These experiments extended over a wide pH range, and Haas et al. (21) modeled the results by invoking binding of the uranyl cation and a uranyl-hydroxide species onto the bacterial surface. However, both uranyl hydroxide and uranyl carbonate complexes were present in solution in their experiments, so the experimental results alone cannot be used to uniquely determine how much of the adsorption should be ascribed to each type of complex. X-ray absorption spectroscopy offers a more direct view of uranyl-bacterial coordination environments, but studies are limited in number and have not examined uranium binding under pH conditions higher than pH 5 (17, 20).

In this study, we conducted uranium adsorption experiments to determine the identity and thermodynamic stabilities of the important bacterial surface uranium species above pH 5, where the aqueous uranium speciation becomes complex. We measured aqueous uranium adsorption onto *B. subtilis* in the pH range of 1.5–9 in both closed (no CO₂) and open atmospheres, with and without aqueous calcium. We use the adsorption experiments, in conjunction with thermodynamic modeling, to test for the presence of adsorbed uranyl-carbonate and calcium-uranyl-carbonate bacterial surface complexes. We used *B. subtilis*, an aerobic Gram-positive bacterial species, in these experiments because it is a common soil microorganism with well-characterized surface properties (22–24).

Experimental Procedures

Bacterial Growth. *B. subtilis* cells were cultured and prepared following the procedures outlined in previous studies (19, 23), excluding the acid wash step in the cell preparation. Cells were maintained on agar plates consisting of trypticase soy agar with 0.5% yeast extract added. Cells for the

* Corresponding author phone: (574)631-4307; e-mail: dgorman@nd.edu.

adsorption experiments were grown by first inoculating a test tube containing 3 mL of trypticase soy broth and 0.5% yeast extract and incubating it for 24 h at 32 °C. The 3 mL bacterial suspension was then transferred to a 1 L volume of trypticase soy broth, also with 0.5% yeast extract, for another 24 h on an incubator shaker table at 32 °C. Cells were then harvested after reaching the early stationary growth phase, pelleted by centrifugation at 1600g for 15 min, and rinsed seven times with 0.1 M NaClO₄. The bacteria were then repelleted by centrifugation at 5000g for two 30 min intervals to remove excess water and create a wet weight that was used to produce suspensions of known bacterial concentrations. The ratio of this wet weight to dry weight is 5.1:1 (25). Subsequent suspensions of bacteria after washing does not release significant amounts of calcium (Supporting Information) or other cations in solution that would affect the charge on the bacterial surface (25). The washing procedure does not lyse the bacterial cells, nor do the cells sporulate or multiply during the course of the experiments.

Control Experiments. The adsorption and desorption experiments were all conducted as functions of pH and solid/solute ratios in batch reaction vessels at 25 ± 1 °C, using a 0.1 M NaClO₄ electrolyte solution to buffer ionic strength. Bacteria were suspended in a 4.2 × 10⁻⁶ M uranium-bearing electrolyte solution diluted from an acidic 4.2 × 10⁻³ M uranium atomic absorption spectroscopy aqueous standard. The experimental uranium concentration was chosen, based on control experiments, to avoid precipitation of any uranium mineral phases. The initial uranium–bacterial suspension was pH 3.5 for all experiments. Control experiments were performed in the same manner as the bacterial adsorption experiments described next, except without bacteria to test for loss of uranium due to precipitation or adsorption onto the reaction vessel. Control experiments using polypropylene reaction vessels revealed significant uranium loss from solution with starting concentrations above 4.2 × 10⁻⁶ M. We did not observe any significant loss of uranium in 4.2 × 10⁻⁶ M control experiments run in Teflon reaction vessels, so all subsequent experiments were conducted using this material.

U Adsorption Experiments. For the bacteria-bearing experiments, we divided the bacterial suspension into separate 10 mL Teflon centrifuge tubes and adjusted the pH of the solution in each to be between pH 1.5 and 9 using small volumes (less than 1% of total volume) of concentrated NaOH and HNO₃. Kinetics experiments (Supporting Information) and previous studies (26) indicated that steady-state adsorption was reached within 30 min and persisted for at least 24 h, and so to ensure the attainment of equilibrium in the remaining adsorption experiments, the reaction vessels were slowly agitated end-over-end for 2 h. Prior to sampling of the experimental fluids, the equilibrium pH was measured in each vessel. Samples were centrifuged for 15 min at 10 000g to pellet the bacteria. Approximately 6 mL of solution was pipetted off the top of the supernatant so as not to disturb the bacterial pellet, and each sample was acidified with 15 μL of concentrated HNO₃ to maintain the uranium in solution prior to analysis. Calcium-bearing experiments were conducted in a similar manner, except 10 mM calcium nitrate was added to the parent solution that contained bacteria and uranium prior to pH adjustment. Analysis for the total aqueous uranium and calcium concentrations in the supernatant of each sample was performed by inductively coupled plasma optical emission spectroscopy with matrix-matched standards with an analytical uncertainty of ±3.5%. Open and closed atmosphere experiments were conducted following the same procedures, except that the open atmosphere experiments were conducted with solutions in equilibrium with atmospheric CO₂, whereas CO₂ was excluded from the closed atmosphere experiments by conducting the experiments in a glovebox purged with a 95% N₂,

5% H₂ gas mixture atmosphere. We used a Coy Model 10 gas analyzer to verify the glovebox atmospheric composition. Glovebox atmospheric preparation entailed purging the box until the oxygen levels were down to 100 ppm, then using a Plas-lab anaerobic chamber catalyst heater until oxygen levels were 0 ppm. In addition, all solutions used in the closed atmosphere experiments were purged for 1 h with N₂ immediately prior to use.

U Desorption Experiments. These experiments were conducted with 0.125 g/L bacteria in the presence and absence of CO₂. An initial adsorption step was conducted in which a U-bacteria parent solution, prepared as described previously, was adjusted to pH 6.3 in an open atmosphere system and to pH 7.1 in a CO₂-free system, and each system was allowed to equilibrate for 2 h. Aliquots of these two parent solutions were placed into separate reaction vessels and subsequently adjusted to higher and lower pH conditions to promote U desorption from the bacteria. The systems were allowed to reequilibrate for an additional 2 h. Samples were taken from these vessels, and U concentrations were determined, as described previously.

Ca Adsorption Experiments. Adsorption experiments were conducted to determine the extent of Ca adsorption onto the bacteria in the absence of U and to constrain the thermodynamic stabilities of the important Ca–bacterial surface complexes. Fowle and Fein (26) conducted similar Ca adsorption experiments, but they used an acid-wash procedure that may have affected the cell wall adsorption properties (24). In this study, a Ca–bacterial parent solution in 0.1 M NaClO₄, with 10 g/L bacteria (wet weight) and 15 ppm Ca, was prepared similar to the U-bacterial parent solution previously described. We divided the bacterial suspension into separate 10 mL Teflon centrifuge tubes and adjusted the pH of the solution in each to be between pH 2 and 9 using small volumes of concentrated NaOH and HNO₃. The reaction vessels were slowly agitated end-over-end for 2 h. Prior to sampling of the experimental fluids, the equilibrium pH was measured in each vessel. Samples were filtered with 0.45 μm nylon membranes, and the supernatant was acidified with 15 μL of 15 M HNO₃. The Ca concentration was determined by ICP–OES. Ca-release control experiments were also conducted to determine if Ca is released from the bacterial cells during experimentation, affecting the total Ca in the experimental systems. The control experiments were performed in a similar manner as the Ca adsorption experiments except without aqueous Ca present. Results, shown in the Supporting Information, indicate that Ca release to solution is negligible under the experimental conditions.

Modeling of Metal–Bacteria Adsorption. We applied a surface complexation approach to model the adsorption of U and Ca onto the *B. subtilis* cells. A surface complexation approach quantifies adsorption using balanced chemical equations. This approach enables prediction of adsorption in systems not directly measured in the laboratory. Using the model of Fein et al. (24) to describe the proton-active sites on the bacterial surface, proton binding is ascribed to four distinct reactions of the following stoichiometry:



where R is a bacterium to which a proton-active functional group type, Li, is attached. Fein et al. (24) use potentiometric titration data to constrain the site concentrations and acidity constants for the pertinent protonation reactions, and we employed their discrete pK_a 4-site nonelectrostatic model with pK_a values of 3.3, 4.8, 6.8, and 9.1. Electrophoretic mobility measurements of *B. subtilis* cells demonstrate that the bacteria exhibit a negative surface charge above pH 2, with increasing negative charge with increasing pH. These observations are consistent with successive deprotonation

of bacterial surface sites with increasing pH and suggest that neither Na^+ from the electrolyte nor elements such as Ca and Mg that may be released to some extent from the cell wall significantly affect the bacterial surface charge under the conditions of the experiments. X-ray absorption spectroscopy (XAS) results (20, 27) suggest that the L1 and L2 sites, with pK_a values of 3.3 and 4.8, are likely phosphoryl and carboxyl groups, respectively. The identities of the other surface sites, with pK_a values of 6.8 and 9.1, are more uncertain, and we refer to them as site 3 (L3) and site 4 (L4), respectively.

We tested the ability of a range of reaction stoichiometries to account for the observed adsorption behavior and used the program FITEQL (28) to determine the model that best fits the experimental data. Although we have no spectroscopic data to help constrain the dominant binding mechanisms above pH 5, adsorption measurements conducted as a function of pH and solute/sorbent ratio provide constraints on the stoichiometry and thermodynamic stability of the important bacterial surface species.

A generic metal adsorption reaction can be represented with the balanced chemical equation



where Li represents one of the four surface functional group types present on the bacterial surface and z can equal 0 or 1. We tested a range of possible reaction stoichiometries and solved for each proposed stability constant as defined by

$$K = \frac{[\text{R-LiH}_z\text{-M}^{(z-1+m)}]}{a_{\text{M}^{m+}} [\text{R-LiH}_z^{(z-1)}]} \quad (3)$$

where a represents the aqueous activity of the subscripted species, and the brackets represent surface site concentrations in moles per kilogram of solution. Activity coefficients are calculated by FITEQL using the Davies equation (28).

Results and Discussion

Adsorption and Desorption Results. Bacteria-free control experiments do not exhibit any measurable loss of U in the open or closed system from pH 1.5 to 9 (not shown). In the CO_2 -free experiments, uranium adsorption increases with increasing pH up to approximately pH 5–6 for each of the three bacterial concentrations studied, reaching adsorption plateaus above approximately pH 6 (Figure 1). The system containing 0.125 g/L bacteria displays a slight decrease in adsorption above pH 8. In the open-atmosphere experiments (Figure 2), we observed similar low pH increases in adsorption with increasing pH to approximately pH 6. However, at higher pH values, each system studied exhibits a significant decrease in adsorption with increasing pH, with more pronounced decreases in the systems with lower bacterial concentrations. The calcium-bearing experiments exhibit no measurable loss of calcium, which is expected under high Ca concentrations combined with the low affinity for Ca to adsorb onto the bacterial surface. The Ca-bearing data exhibit similar increases in adsorption with increasing pH to approximately pH 6. However, above pH 6, the presence of the calcium leads to dramatically enhanced adsorption relative to the open-atmosphere calcium-free systems. Each calcium-bearing system exhibits a decrease in adsorption above pH 6, but the decrease is less than that observed for the open atmosphere calcium-free systems. As expected in all three systems, we observe an increase in adsorption as bacterial concentrations increase.

All three systems exhibit extensive uranium adsorption onto *B. subtilis* over the entire pH range studied, including to pH values below 2. The extensive adsorption observed

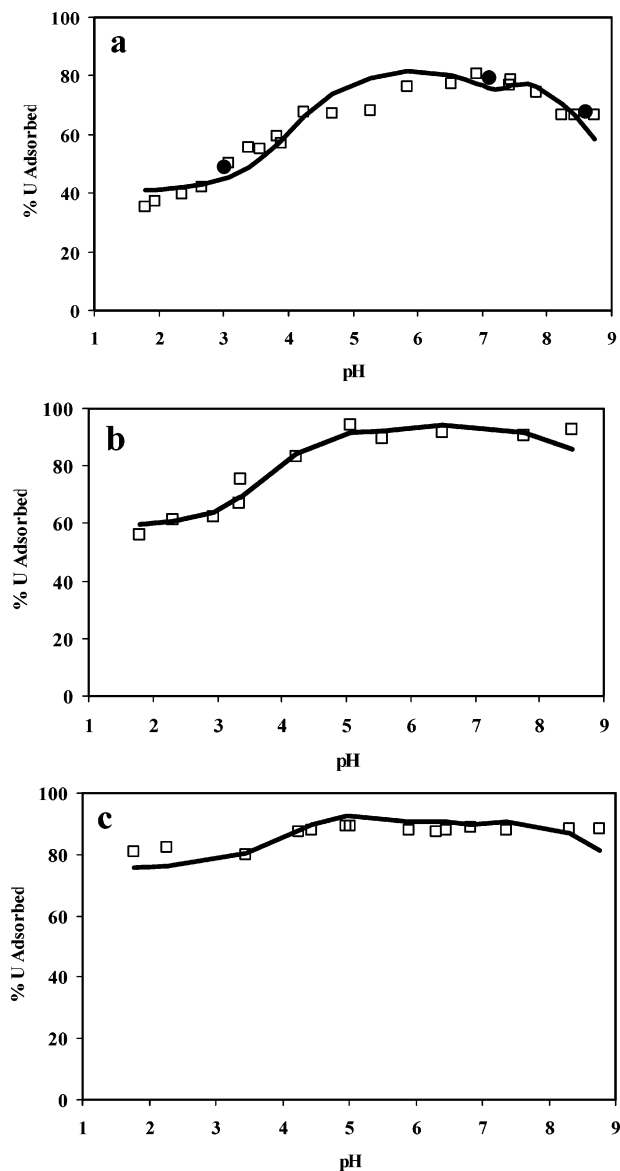


FIGURE 1. U adsorbed by *B. subtilis* as a function of pH and bacterial concentration, (a) 0.125, (b) 0.25, and (c) 0.5 g/L (wet weight), in a closed system (no CO_2). The curve (—) represents the best-fit surface complexation model (see text). Closed circles represent results from desorption experiments conducted with an initial adsorption step at pH 7.1.

under low pH conditions, consistent with the observations by Fowle et al. (19) and Haas et al. (21), is in contrast to the typically low levels of adsorption documented for other aqueous cations under similar conditions (23). Potentiometric titrations and electrophoretic mobility experiments both indicate that below pH 2–3, bacterial surface sites exist dominantly in their protonated, neutral states, greatly diminishing the electrostatic contribution driving cation adsorption (24). The high degree of low pH uranium adsorption suggests that electrostatic forces alone cannot explain the adsorption mechanism and that covalent bonding likely contributes significantly to the adsorption reaction energetics.

The high extent of adsorption that occurs at mid-pH values is likely due to a range of adsorption reactions because the aqueous speciation of uranium is so complex in this pH range. The importance of the uranyl ion in the aqueous uranium budget diminishes dramatically above pH 4, with uranyl-hydroxide and uranyl-carbonate complexes dominating

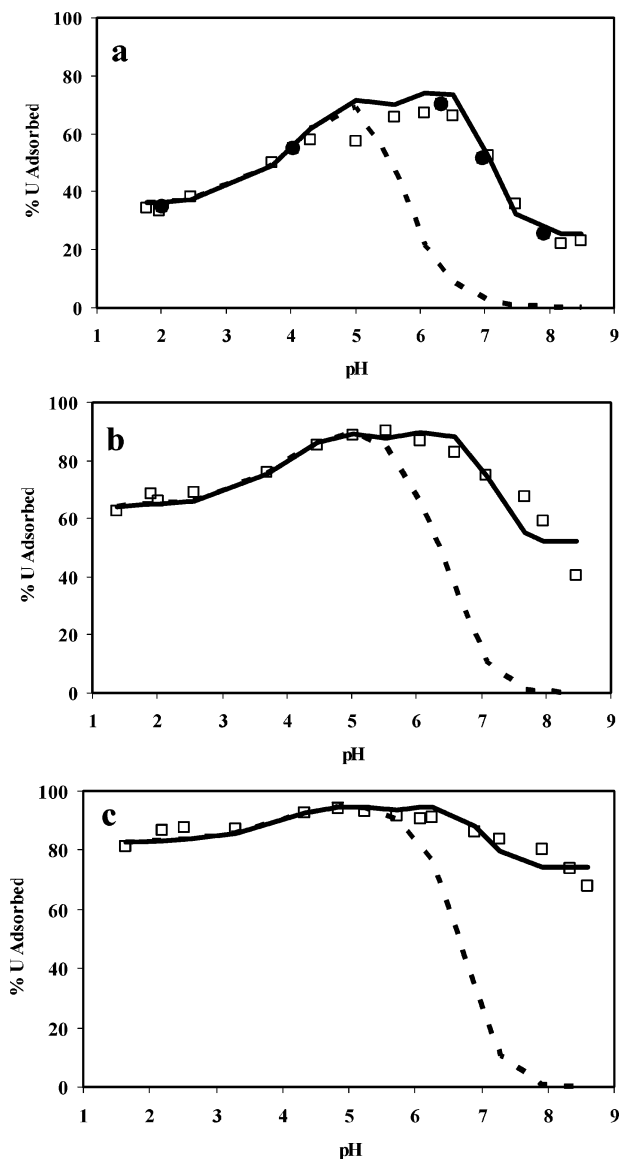


FIGURE 2. U adsorbed by *B. subtilis* as a function of pH and bacterial concentration, (a) 0.125, (b) 0.25, and (c) 0.5 g/L (wet weight), in an open system. The dashed curve (---) represents the predicted adsorption in the absence of uranyl carbonate surface complexation. The solid curve (—) represents the best-fit surface complexation model (see text). Closed circles represent results from desorption experiments conducted with an initial adsorption step at pH 6.3.

above pH 5. The adsorption data do not mimic the decrease in activity of uranyl ion above pH 4, strongly suggesting that the other uranium complexes adsorb onto the bacterial surface to a significant extent. Under the highest pH conditions studied here in calcium-free and -bearing open atmosphere experiments, the extent of adsorption, although diminished somewhat by aqueous uranyl-carbonate and calcium-uranyl-carbonate complexation, is not diminished nearly as dramatically as is the case for mineral surfaces (4–7). The relatively high extent of adsorption under these high pH conditions is likely caused by adsorption of the uranyl aqueous complexes themselves onto the bacterial surface. Although adsorption of uranyl-carbonate complexes onto mineral surfaces has been reported recently (13, 14, 16), adsorption of these negatively charged aqueous uranyl complexes onto a highly negatively charged bacterial surface is particularly surprising and must reflect adsorption energetics that can overcome the high forces of electrostatic repulsion.

Desorption experiments were conducted to determine the reversibility of the U-bacteria adsorption reactions. Figures 1a and 2a depict results from desorption experiments in which a parent solution containing a U-bacterial suspension was adjusted to a pH where maximum adsorption occurs and allowed to reach an initial adsorption equilibrium. We sampled the solution after this initial adsorption step and observed that approximately 80 and 70% of the U was bound to the bacteria in the CO₂-free and open atmosphere systems, respectively. Next, we took aliquots of this solution, adjusted the pH to lower and higher values, and allowed these aliquots to reequilibrate by desorbing U from the cell walls. As shown in Figures 1a and 2a, the desorption data points exhibit excellent agreement with the adsorption measurements, providing tight constraints on the pH adsorption edge. This agreement indicates that the bacterial U adsorption reactions, like those of many other aqueous cations (26), are completely reversible over the time period of the experiments. These observations, in combination with previous XAS studies (20), further suggest that our adsorption measurements reflect equilibrium conditions for U partitioning between the aqueous phase and the bacterial cell walls rather than U penetration into the cytoplasm of the cell.

The calcium adsorption experiments (without U present) indicate that Ca does not adsorb nearly as extensively onto the cell wall as does U. Adsorption is low under low pH conditions and increases slightly with increasing pH. Maximum adsorption occurs above pH 6 and remains constant above this pH with 24% of the total Ca adsorbed (see Supporting Information).

Modeling Results. Although we have no spectroscopic data to help constrain the important binding mechanisms, adsorption measurements conducted as a function of equilibrium pH and solute/sorbent ratio can provide constraints on the stoichiometry and thermodynamic stability of the important bacterial surface species. Our approach was to model the simplest conditions first and to use those results as a foundation for models of the more complex systems. Therefore, we first modeled the low pH data in all of the systems because under low pH conditions, the aqueous U speciation is dominated by the uranyl ion alone. Then, we continued by modeling sequentially higher pH data, starting first with the CO₂-free system, progressing to the open atmosphere calcium-free system, and finishing with the open atmosphere calcium-bearing system. We used the program FITEQL (28) to construct models involving different uranium adsorption reactions and to determine the model that most accurately describes the observed adsorption behavior. In each calculation, we accounted for aqueous uranyl speciation using the reactions and stability constants for the important uranyl aqueous species listed in Table 1 of the Supporting Information.

The model that best fits the low pH data is a two-site model with uranyl adsorbed onto protonated L4 sites and onto deprotonated L2 sites. Binding onto the protonated L4 site is used as a surrogate for adsorption onto a hypothetical site whose pK_a is lower than those determined by Fein et al. (26). Invoking this surrogate site is necessary in the model to account for the significant U adsorption that occurs at pH values below the pK_a of site 1. Under these low pH conditions, the bacterial cell wall is still proton-active, which suggests the presence of this additional site (26). However, because the pK_a and site concentration of this hypothetical site are unknown, it is impossible to model U adsorption onto it. As a surrogate for binding onto this hypothetical lowest pK_a site, we represent this reaction by including adsorption of U onto the protonated form of site 4 in our model. Although it is unlikely that U actually binds onto a protonated site, the protonated site serves as a good surrogate because its

TABLE 1

reaction		log $K \pm 2\sigma$
U Surface Complexation Reactions		
1	$\text{UO}_2^{2+} + \text{R}^a\text{-HL4}^0 \leftrightarrow \text{R-HL4-UO}_2^{2+}$	5.4 ± 0.2
2	$\text{UO}_2^{2+} + \text{R-L2}^- \leftrightarrow \text{R-L2-UO}_2^{2+}$	6.2 ± 0.3
3	$\text{UO}_2\text{OH}^+ + \text{R-L3}^- \leftrightarrow \text{R-L3-UO}_2\text{OH}^0$	7.1 ± 0.4
4	$(\text{UO}_2)_3(\text{OH})_7^- + \text{R-L4}^- \leftrightarrow \text{R-L4-(UO}_2)_3(\text{OH})_7^{2-}$	8.6 ± 0.6
5	$\text{UO}_2\text{CO}_3^0 + \text{R-L2}^- \leftrightarrow \text{R-L2-UO}_2\text{CO}_3^-$	5.5 ± 0.6
6	$(\text{UO}_2)_2\text{CO}_3(\text{OH})_3^- + \text{R-L3}^- \leftrightarrow \text{R-L3-(UO}_2)_2\text{CO}_3(\text{OH})_3^{2-}$	7.5 ± 0.6
7	$\text{UO}_2(\text{CO}_3)_3^{4-} + \text{L3}^- \leftrightarrow \text{R-L3-UO}_2(\text{CO}_3)_3^{5-}$	7.3 ± 0.6
8	$\text{Ca}_2\text{UO}_2(\text{CO}_3)_3^0 + \text{R-L2}^- \leftrightarrow \text{R-L2-Ca}_2\text{UO}_2(\text{CO}_3)_3^-$	5.0 ± 0.2
Aqueous Complexation Reactions for Ca-Bearing System		
9	$\text{UO}_2^{2+} + 3\text{CO}_3^{2-} + 2\text{Ca}^{2+} \leftrightarrow \text{Ca}_2\text{UO}_2(\text{CO}_3)_3$	30.45^b
10	$\text{Ca}^{2+} + \text{HCO}_3^- \leftrightarrow \text{CaHCO}_3^+$	1.11^c
11	$\text{Ca}^{2+} + \text{CO}_3^{2-} \leftrightarrow \text{CaCO}_3^0$	3.22^c
Ca Surface Complexation Reactions		
12	$\text{R-L1}^- + \text{Ca}^{2+} \leftrightarrow \text{R-L1-Ca}^+$	2.7 ± 0.1^d
13	$\text{R-L2}^- + \text{Ca}^{2+} \leftrightarrow \text{R-L2-Ca}^+$	2.5 ± 0.1^d

^a R is a bacterium to which a functional group type, Li, is attached. ^b From ref 29. ^c From ref 31. ^d This paper (Supporting Information).

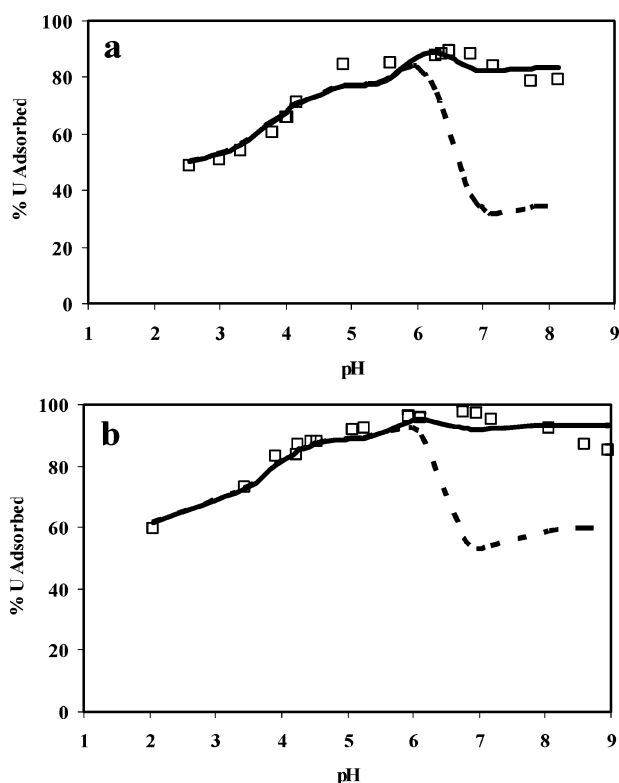


FIGURE 3. U adsorbed by *B. subtilis* as a function of pH and bacterial concentration, (a) 0.125 and (b) 0.25 g/L (wet weight), in an open system with 10 mM Ca. The dashed curve (---) represents predicted adsorption in the absence of calcium uranyl carbonate surface complexation. The solid curve (—) represents the best-fit surface complexation model (see text).

concentration, like that of the deprotonated form of the lowest hypothetical pK_a site, does not change over the low pH range where adsorption is observed. As a function of pH and bacterial concentration, this model provides an excellent fit to all data from all systems below pH 5. The log K values for these U-bacterial complexes are reported with their 2σ errors as reactions 1 and 2 in Table 1. As stated previously, we used all of the data below pH 5 from each of the eight experimental systems (Figures 1–3) to constrain these values and associated uncertainties. Each dataset (where a dataset is defined as data collected as a function of pH for a particular bacterial concentration for a particular system of interest) yields a set

of best-fitting K values for these reactions. The K values reported in Table 1 are the averages of these calculated values, weighted to account for the number of data points in each dataset. The errors were determined by determining the range of log K values about these averages that results in models that encompass 95% of the data in the pH range of interest. This model is similar to that used by Fowle and Fein (19) in that each invokes uranyl adsorption onto protonated phosphoryl and deprotonated carboxyl sites. However, the calculated K values cannot be directly compared between these two studies because the two studies used different models for the protonation behavior of the bacterial cell wall, and the choice of model directly affects calculated K values for metal adsorption reactions.

We used our calculated stability constants for the low pH uranyl–bacterial species to predict the extent of adsorption under higher pH conditions in the CO_2 -free system. The two-site model underestimates the observed extent of adsorption above pH 5, likely because it only involves UO_2^{+2} adsorption and neglects adsorption of the uranyl–hydroxide complexes that dominate the aqueous speciation above pH 5. Keeping the calculated stability constants from the two-site model fixed, we tested the ability of models involving the adsorption of uranyl–hydroxide species onto deprotonated bacterial surface sites to account for the higher pH data. As an extension of our approach to modeling the low pH data, we considered sequentially higher pH ranges, including in the model additional uranyl–hydroxide bacterial surface complexes as we proceed. The data to pH 7.5 allowed us to determine the stability of one uranyl–hydroxide bacterial surface complex; adding the data to pH 9 required the inclusion of an additional uranyl–hydroxide bacterial surface complex to the model. We tested various models involving different uranyl hydroxide species depending on their abundance in solution at the particular pH range where our model did not fit. Thus, the best-fit model for uranium adsorption in the CO_2 -free system (reactions 1–4 in Table 1) involves the formation of four distinct uranyl–bacterial surface complexes and can successfully account for the observed adsorption behavior across the pH range of this study and as a function of bacterial concentration in the CO_2 -free systems (Figure 1). The log K values listed in Table 1 and their 2σ uncertainties are calculated as described previously for reactions 1 and 2 in Table 1, with K values averaged for the three bacterial concentration datasets depicted in Figure 1.

To model the open atmosphere, Ca-free experiments, we used the bacterial adsorption reactions and associated K values from the CO_2 -free experiments to estimate the extent

of adsorption expected in the CO₂-bearing system (Figure 2). These calculations accounted for aqueous uranyl-carbonate complexation using the stability constants for these reactions that are listed in Table 1 of the Supporting Information. This initial model was calculated assuming that no surface complexation of the uranyl carbonate species occurred. The bacterial surface complexes defined from the CO₂-free model reasonably describe adsorption in the low- to mid-pH range for the open atmosphere experiments; however, the model underestimates the extent of adsorption dramatically at higher pH values (Figure 2). This is strong evidence that uranyl-carbonate species, which dominate uranyl speciation under these higher pH conditions, adsorb onto the bacterial surface and are responsible for the enhanced adsorption relative to the estimated amount. Using the CO₂-free model as our baseline model, we tested the ability of models involving the adsorption of various uranyl-carbonate species to account for the observed bacterial adsorption. As we did in modeling the CO₂-free system, we started with the lower pH data, constrained the thermodynamic stability of the uranyl-carbonate bacterial surface complex that best accounted for those, and sequentially repeated the process with increasing pH. This process yielded a model for the open-atmosphere data that includes three uranyl-carbonate bacterial surface complexes in addition to the four reactions from the CO₂-free model (reactions 1–4 in Table 1). The overall model provides a good fit to the observed adsorption behavior in the open-atmosphere experiments over the entire pH range and for all bacterial concentrations studied. The uranyl-carbonate bacterial surface complex reactions and their log *K* values are reported with their 2σ errors as reactions 5–7 in Table 1. The log *K* values are averaged as described previously, with weighted average *K* values determined from the three bacterial concentration datasets depicted in Figure 2.

For the calcium-bearing systems, the pertinent aqueous Ca complexation reactions (reactions 9–11 in Table 1) and Ca-bacterial complexation reactions (reactions 12 and 13 in Table 1, data shown in Supporting Information) were taken into account during modeling. We modeled Ca adsorption by first testing a model involving Ca adsorption onto a deprotonated site 1 (L1⁻). This model accounts for the observed adsorption up to approximately pH 4.8 but significantly underestimates the extent of adsorption at higher pH. To account for the underestimation above pH 4.8, we added an additional reaction to the model to account for Ca adsorption onto a deprotonated site 2 (L2⁻). This two-site model provides an excellent fit to the data over the entire pH range of the experiments (see Supporting Information). The log *K* values are reported as reactions 12 and 13 in Table 1, with their 2σ error, calculated by determining the range of log *K* values that encompasses 95% of the experimental data.

We used a similar modeling approach to that applied to the open atmosphere, Ca-free systems, to model the open atmosphere Ca-bearing system. That is, we used the bacterial adsorption reactions and associated *K* values from the CO₂-free and open atmosphere experiments (reactions 1–7 in Table 1) to estimate the extent of adsorption expected in the calcium-bearing system. The calculation of this initial model accounted for aqueous calcium-uranyl-carbonate complexation using the stability constant from Bernhard et al. (29) (reaction 9 in Table 1). This initial model was calculated assuming that no surface complexation of the calcium-uranyl-carbonate species occurs with the bacterial surface. The bacterial surface complexes defined from the CO₂-free and open atmosphere systems (reactions 1–7 in Table 1) reasonably describe adsorption in the low- to mid-pH range for the calcium-bearing experiments. However, the model dramatically underestimates the observed extent of adsorp-

tion at higher pH values (Figure 3), providing strong evidence that the calcium-uranyl-carbonate complex, which dominates the uranyl speciation under these higher pH conditions, adsorbs onto the bacterial surface and is responsible for the enhanced adsorption relative to the estimated amount. The inclusion of 10 mM Ca(NO₃)₂ in these Ca-bearing experiments slightly increases the ionic strength of this system relative to the Ca-free systems; however, the effect of this ionic strength increase is likely to be small and cannot account for the observed enhanced adsorption in the presence of aqueous Ca. Typically, increasing the ionic strength of a system causes the extent of adsorption to decrease due to the collapse of the electric double layer on the adsorbing surface. In our system, we see the opposite effect, with adsorption increasing with the addition of Ca.

To account for the enhanced adsorption behavior relative to the model, we tested model fits involving calcium-uranyl-carbonate complex adsorption onto sites L2⁻, L3⁻, and L4⁻. The model involving the L2⁻ binding site alone yields a reasonable fit to the observed adsorption behavior both as a function of pH and as a function of bacterial concentration (Figure 3). The surface complexation reaction, its average log *K* value, and associated 2σ uncertainty are reported in Table 1 as reaction 8. The averaged log *K* value with associated uncertainty is determined as described previously, with a weighted average *K* value determined from the two bacterial concentration datasets depicted in Figure 3.

Our experimental approach, which measured adsorption in both CO₂-free and open atmosphere systems, is the first to provide constraints on the effect of CO₂ and calcium on bacterial adsorption of uranium, and the modeling approach that we used enabled us to differentiate between uranyl-hydroxide and uranyl-carbonate adsorption. Our results suggest that neutrally and negatively charged uranyl-hydroxides, uranyl-carbonates, and the calcium-uranyl-carbonate complex form highly stable surface complexes on the negatively charged *B. subtilis* surface, leading to significantly enhanced adsorption in the pH range of 7–9. The presence of these surface complexes is unexpected given the unfavorable electrostatic energetics between the aqueous uranyl complexes and the bacterial surface. Clearly, electrostatic interactions alone cannot account for the observed adsorption behavior. Some other driving force for the adsorption, such as that of covalent bonding, must also be present for highly negatively charged aqueous complexes to adsorb onto the negatively charged bacterial surface to the extent observed.

The stability constants of the important uranium-bacterial surface complexes that we determined in this study may help predict U adsorption onto other bacterial species (30) and can be incorporated into geochemical models that will help determine the potential impact of bacterial surface adsorption on the mobility of uranium in groundwater systems. Such modeling can be used to assess and predict the effects of pH, CO₂, and calcium concentration on the uranium adsorption behavior. Our discovery of uranyl-carbonate and calcium-uranyl-carbonate adsorption onto a common bacterial surface suggests that uranium may not be as mobile as is currently thought in CO₂- and calcium-bearing systems, a result that may force reconsideration of remediation and retardation strategies for uranium contamination in circumneutral bacteria-bearing aerobic systems.

Acknowledgments

Research funding was provided by the National Science Foundation through an Environmental Molecular Science Institute grant (EAR02-21966). Three journal reviews, and the comments of Editor Janet Hering, significantly improved the quality and presentation of the manuscript.

Supporting Information Available

Kinetics data, bacterial Ca and P release data, Ca adsorption data and modeling, and U(VI) aqueous phase reactions used in modeling our data. This material is available free of charge via the Internet at <http://pubs.acs.org>.

Literature Cited

- (1) Zhang, P.-C.; Krumhansl, J. L.; Brady, P. V. Introduction to properties, sources, and characteristics of soil radionuclides. *SSSA Spec. Publ.* **2002**, *59*, 1–20.
- (2) Nakajima, A.; Horikoshi, T.; Sakaguchi, T. Studies on the accumulation of heavy metal elements in biological systems. XXI. Recovery of uranium by immobilized microorganisms. *Eur. J. Appl. Microbiol. Biotechnol.* **1982**, *16*, 88–91.
- (3) Atun, G.; Kilislioglu, A. The adsorption behavior of natural sand in contact with uranium contaminated seawater. *J. Environ. Sci. Health, Part A* **2002**, *A37*, 1295–1305.
- (4) Hsi, C. K. D.; Langmuir, D. Adsorption of uranyl onto ferric oxyhydroxides: application of the surface complexation site-binding model. *Geochim. Cosmochim. Acta* **1985**, *49*, 1931–1941.
- (5) Lieser, K. H.; Thybusch, B. Sorption of uranyl ions on hydrous titanium dioxide. *Fresenius' J. Anal. Chem.* **1988**, *332*, 351–357.
- (6) Lieser, K. H.; Quandt-Klenk, S.; Thybusch, B. Sorption of uranyl ions on hydrous silicon dioxide. *Radiochim. Acta* **1992**, *57*, 45–50.
- (7) Waite, T. D.; Davis, J. A.; Payne, T. E.; Waychunas, G. A.; Xu, N. Uranium(VI) adsorption to ferrihydrite: application of a surface complexation model. *Geochim. Cosmochim. Acta* **1994**, *58*, 5465–5478.
- (8) Giblin, A. M.; Batts, B. D.; Swaine, D. J. Laboratory simulation studies of uranium mobility in natural waters. *Geochim. Cosmochim. Acta* **1981**, *45*, 699–709.
- (9) Yanase, N.; Payne, T. E.; Sekine, K. Groundwater geochemistry in the Koongarra ore deposit, Australia (II). Activity ratios and migration mechanisms of uranium series radionuclides. *Geochem. J.* **1995**, *29*, 31–54.
- (10) Longmire, P.; Turney, W. R.; Mason, C. F. V.; Dander, D.; York, D. Predictive geochemical modeling of uranium and other contaminants in laboratory columns in relatively oxidizing, carbonate-rich solutions. *Technol. Programs Radioact. Waste Manage. Environ. Restor.* **1994**, 2081–2085.
- (11) Turney, W. R.; Mason, C. F. V.; Longmire, P.; Dander, D. C.; York, D. A.; Chisholm-Brause, C. J.; Thomson, B. M. Carbonate heap leach of uranium-contaminated soils. *Technol. Programs Radioact. Waste Manage. Environ. Restor.* **1994**, 2087–2090.
- (12) Buck, E. C.; Brown, N. R.; Dietz, N. L. Contaminant uranium phases and leaching at the Fernald site in Ohio. *Environ. Sci. Technol.* **1996**, *30*, 81–88.
- (13) Bargar, J. R.; Reitmeyer, R.; Davis, J. A. Spectroscopic Confirmation of Uranium(VI)–Carbonate Adsorption Complexes on Hematite. *Environ. Sci. Technol.* **1999**, *33*, 2481–2484.
- (14) Bargar, J. R.; Reitmeyer, R.; Lenhart, J. J.; Davis, J. A. Characterization of U(VI)–carbonate ternary complexes on hematite: EXAFS and electrophoretic mobility measurements. *Geochim. Cosmochim. Acta* **2000**, *64*, 2737–2749.
- (15) Bencheikh-Latmani, R.; Leckie, J. O.; Bargar, J. R. Fate of Uranyl in a Quaternary System Composed of Uranyl, Citrate, Goethite, and *Pseudomonas fluorescens*. *Environ. Sci. Technol.* **2003**, *37*, 3555–3559.
- (16) Stamberg, K.; Venkatesan, K. A.; Vasudeva Rao, P. R. Surface complexation modeling of uranyl ion sorption on mesoporous silica. *Colloids Surf., A* **2003**, *221*, 149–162.
- (17) Hennig, C.; Panak, P. J.; Reich, T.; Rossberg, A.; Raff, J.; Selenska-Pobell, S.; Matz, W.; Bucher, J. J.; Bernhard, G.; Nitsche, H. EXAFS investigation of uranium(VI) complexes formed at *Bacillus cereus* and *Bacillus sphaericus* surfaces. *Radiochim. Acta* **2001**, *89*, 625–631.
- (18) Sar, P.; D'Souza, S. F. Biosorptive uranium uptake by a *Pseudomonas* strain: characterization and equilibrium studies. *J. Chem. Technol. Biotechnol.* **2001**, *76*, 1286–1294.
- (19) Fowle, D. A.; Fein, J. B.; Martin, A. M. Experimental Study of Uranyl Adsorption onto *Bacillus subtilis*. *Environ. Sci. Technol.* **2000**, *34*, 3737–3741.
- (20) Kelly, S. D.; Kemner, K. M.; Fein, J. B.; Fowle, D. A.; Boyanov, M. I.; Bunker, B. A.; Yee, N. X-ray absorption fine structure determination of pH-dependent U-bacterial cell wall interactions. *Geochim. Cosmochim. Acta* **2002**, *66*, 3855–3871.
- (21) Haas, J. R.; Dichristina, T. J.; Wade, R. Thermodynamics of U(VI) sorption onto *Shewanella putrefaciens*. *Chem. Geol.* **2001**, *180*, 33–54.
- (22) Beveridge, T. J.; Murray, R. G. E. Sites of metal deposition in the cell wall of *Bacillus subtilis*. *J. Bacteriol.* **1980**, *141*, 876–887.
- (23) Fein, J. B.; Daughney, C. J.; Yee, N.; Davis, T. A. A chemical equilibrium model for metal adsorption onto bacterial surfaces. *Geochim. Cosmochim. Acta* **1997**, *61*, 3319–3328.
- (24) Fein, J. B.; Boily, J. F.; Yee, N.; Gorman-Lewis, D.; Turner, B. Potentiometric titrations of *Bacillus subtilis* cells and a comparison of modelling approaches. *Geochim. Cosmochim. Acta* **2005**, *69*, 1123–1132.
- (25) Borrok, D.; Fein, J. B.; Tischler, M.; O'Loughlin, E.; Meyer, H.; Liss, M.; Kemner, K. M. The effect of acidic solutions and growth conditions on the adsorptive properties of bacterial surfaces. *Chem. Geol.* **2004**, *209*, 107–119.
- (26) Fowle, D. A.; Fein, J. B. Experimental measurements of the reversibility of metal–bacteria adsorption reactions. *Chem. Geol.* **2000**, *168*, 27–36.
- (27) Boyanov, M. I.; Kelly, S. D.; Kemner, K. M.; Bunker, B. A.; Fein, J. B.; Fowle, D. A. Adsorption of cadmium to *Bacillus subtilis* bacterial cell walls: A pH-dependent X-ray absorption fine structure spectroscopy study. *Geochim. Cosmochim. Acta* **2003**, *67*, 3299–3311.
- (28) Herbelin, A.; Westall, J. C. *FITEQL 3.1, A computer program for determination of chemical equilibrium constants from experimental data, Report 94-01*; Department of Chemistry, Oregon State University: Corvallis, OR, 1994.
- (29) Bernhard, G.; Geipel, G.; Reich, T.; Brendler, V.; Amayri, S.; Nitsche, H. Uranyl(VI) carbonate complex formation: validation of the $\text{Ca}_2\text{UO}_2(\text{CO}_3)_3(\text{aq.})$ species. *Radiochim. Acta* **2001**, *89*, 511–518.
- (30) Borrok, D. M.; Fein, J. B.; Kulpa, C. F., Jr. Cd and proton adsorption onto bacterial consortia grown from industrial wastes and contaminated geologic settings. *Environ. Sci. Technol.* **2004**, *38*, 5656–5664.
- (31) Wolery, T. J. *EQ3NR, a computer program for geochemical aqueous speciation-solubility calculations: theoretical manual, user's guide, and related documentation (Version 7.0), Part 3*; Livermore National Laboratory: Livermore, CA, 1992.

Received for review December 23, 2004. Revised manuscript received April 26, 2005. Accepted April 27, 2005.

ES047957C